Proceedings of COMP07:
6th International Symposium on Advanced Composites
16-18 May, 2007, Corfu, Greece

COMP2007-033

CONSTITUTIVE MODELING OF MAGNETIC SHAPE MEMORY ALLOYS WITH MAGNETO-MECHANICAL COUPLING

Dimitris C. Lagoudas
Department of Aerospace Engineering
Texas A&M University
College Station, Texas 77843-3141
Email: d-lagoudas@ tamu.edu

Bjoern Kiefer
Alicia J. Broederdorf
Department of Aerospace Engineering
Texas A&M University
College Station, Texas 77843-3141

ABSTRACT

Following up on previous work by the authors, which develops a methodology for interpreting data accurately for magnetic shape memory alloys (MSMAs), the coupling between the mechanical and magnetostatic problems is investigated by considering the influence of magnetic body force on the equilibrium equations. The magnetic body force is computationally evaluated using a multiphysics FEA over the domain of a MSMA specimen with a rectangular cross-section, subjected to applied mechanical and magnetic boundary conditions. The analysis presented in this paper is useful in interpreting experimental data necessary for calibration and validation of reliable constitutive models for magnetic shape memory alloys.

1. INTRODUCTION

Magnetic shape memory alloys are able to produce large field-induced strains (MFIS), making them a main topic of research [1-7] since the MFIS are at least one order of magnitude higher than those of ordinary magnetostrictive materials. These inelastic strains are obtainable at frequencies of up to 1 kHz, a much greater frequency when compared to the temperature- or stress- induced strain in conventional shape memory alloys (SMAs). Martensitic variants within the material rearrange themselves due to applied magnetic fields, which cause an observed nonlinear, hysteretic, stress-dependent strain response. The shape change is coupled to a nonlinear change of the magnetization which changes through the mechanisms of magnetic domain wall motion and the local rotation of magnetization vectors.

Previous work by the authors has mainly concentrated on the development of a continuum level constitutive model for MSMAs [8-11], with more recent work focusing on solving magnetostatic boundary value problems for the accurate interpretation of experimental results [12,13] which are necessary for model validation. The material behavior of the MSMAs is based on the magnetic field within the specimen. However, this is hard to directly measure and due to the demagnetization effect, is different from the applied field outside of the specimen. The magnetization of the specimen is nonuniform due its geometry. Therefore, techniques involving the use of demagnetization factors only lead to approximate solutions of the internal magnetic field. This paper examines the coupling between the mechanical and magnetostatics problem through the body forces and body couples within the equilibrium equations of the magnetostatic boundary value problem previously outlined by the authors [12,13]. The thermodynamics-based phenomenological model developed by the authors is used to determine the magnetization response of the MSMA sample for input to the magnetostatic problem.

2. THE MAGNETOMECHANICAL BOUNDARY VALUE PROBLEM

In the following paragraphs basic concepts of magnetostatics in the presence of magnetized matter are summarized to provide the foundation for the analysis of magnetostatic boundary value problems (BVPs) for MSMA materials. For static conditions in stationary bodies and negligible free currents, Maxwell's equations in $\mathbb{R}^3$, the space occupied by the magnetized body and the infinite surrounding free space, reduce to [14,15]

$$\nabla \cdot \mathbf{B} = 0 \text{ and } \nabla \times \mathbf{H} = 0 \text{, in } \mathbb{R}^3, \qquad (1)$$

where **B** is the magnetic flux density and **H** is the magnetic field strength. These two quantities are related through the constitutive relation $\mathbf{B} = \mu_o(\mathbf{H} + \mathbf{M})$, in which μ_o is the permeability of free space and **M** is the magnetization. The magnetization is defined at all material points within the magnetized body, in this case the magnetic shape memory alloy sample. The field variables that result from the solution of Eqns. (1) are subject to the jump conditions

$$[[\mathbf{B}]] \cdot \mathbf{n} = 0 \text{ and } [[\mathbf{H}]] \times \mathbf{n} = 0, \qquad (2)$$

on all interface, where surface currents have again been considered negligible. The jump of a generic field A is defined as $[[\mathrm{A}]] = \mathrm{A}^+ - \mathrm{A}^-$. The sign superscript refers to the direction of the unit normal **n**. As a consequence the normal component of the flux density and the tangential component of the field strength have to be continuous over any interface.

Taking advantage of the specific form of Eqns. (1), the magnetostatic problem is often reformulated by deriving the magnetic field strength from a scalar potential or the flux density from a vector potential. In the latter case $\mathrm{B} = \nabla \times \mathrm{A}$ identically satisfies the first Gauss' law, which is the first equation in (1). Using the identity $\nabla \times (\nabla \times \mathrm{A}) = \nabla(\nabla \cdot \mathrm{A}) - \Delta \mathrm{A}$, and the Coulomb gauge $\nabla \cdot A = 0$ [14], the second equation in (1), known as Ampére's law, takes the form

$$\nabla \times \left(\mu_o^{-1} \nabla \times \mathbf{A} - \mathbf{M} \right) = 0, \text{ or } \Delta \mathbf{A} = -\mu_0 \nabla \times \mathbf{M}, \text{ in } \mathbb{R}^3, \qquad (3)$$

which is the vector-values Poisson equation for the magnetic potential **A.** Δ denotes the vector-valued Laplace operator.

As a consequence of the Eqns. (1) and (2), a magnetic body is subjected to the magnetostatic field caused by its own magnetization is such a manner that it tends to demagnetize it. This demagnetization effect has relevance when measuring the magnetization response of magnetic materials, since the resulting difference between the externally applied field and internal magnetic fields makes experimental data difficult to interpret. Generic integral representations of the magnetic field as resulting from Eqns. (1) exist [14,16]. For uniformly magnetized bodies the magnetization vector can be taken outside the integral, which then takes the form

$$\mathbf{H}(\mathbf{r}) = -\left[\frac{1}{4\pi} \iint_{\partial\Omega} \frac{\mathbf{r} - \mathbf{r}'}{|\mathbf{r} - \mathbf{r}'|^3} \otimes \mathbf{n}' \, dA' \right] \mathbf{M} = \text{-}\mathbf{DM} \ , \qquad (4)$$

where **r** is the position at which **H** is evaluated in $\mathbb{R}^3$ and $\mathbf{r}'$ the location of a point on the surface $\partial\Omega$, with unit outward normal $\mathbf{n}'$, of the region Ω occupied by the magnetized body. By applying the divergence theorem an equivalent volume integral representation of Eqn. (4) can be obtained. The magnetic field caused by a magnetized body of known uniform magnetization can thus be computed by simply multiplying the magnetization vector with the demagnetization tensor **D**, which only depends on the geometry of the body and can be computed by evaluating the bracketed integral expression in Eqn. (4). The demagnetization tensor has the following properties: i) it is independent of position inside an ellipsoidal body; ii) it is diagonal if its eigenvectors are aligned with the symmetry axes of the body; iii) its trace is 1, if evaluated inside the body. It has been computed and tabularized for a number of standard geometries and numerical solution schemes have been provided for non-ellipsoidal shapes [17-21].

For uniformly magnetized samples of arbitrary shape average demagnetization factors are defined. If additionally an external field $\mathbf{H}^{\text{applied}}$ is applied, superposition leads to the following expression for the average magnetic field inside a non-elliposoidal body with uniform magnetization

$$\langle \mathbf{H} \rangle = \mathbf{H}^{applied} - \langle \mathbf{D} \rangle \mathbf{M} \qquad (5)$$

By definition the demagnetization factor loses its meaning for bodies with nonuniform magnetization. In Eqn. (5) the uniformity of **M** was simply assumed. However, the magnetization induced in a non-ellipsoidal body by an external field is always nonuniform unless magnetic saturation is reached everywhere in the body at high fields. Furthermore, if the magnetization is a function of the applied field the magnetostatic problem as described by Eqn. (3) becomes nonlinear and superposition no longer holds. Thus, for the nonlinear problem involving a magnetized sample of non-ellipsoidal shape whose

magnetization is a function of the magnetic field, an explicit numerical solution of the magnetostatic boundary value problem has to be obtained. For MSMAs the problem is complicated by the fact that the magnetic properties are nonlinear, hysteretic and stress-level dependent and that the shape of the sample changes due to the magnetic field-induced strain. The latter aspect, however, is expected to have negligible influence.

In addition to the magnetostatic equations, the boundary value problem is governed by the mechanical equations, namely the conservation of linear and angular momentum for the magnetic continuum [22,23].

$$\nabla \cdot \sigma + \rho \mathbf{f} + \rho \mathbf{f}^{\mathbf{m}} = 0 \quad \text{in } \Omega, \tag{6a}$$

$$\operatorname{skw} \sigma = \rho \mathbf{L}^{m} \quad \text{in } \Omega, \tag{6b}$$

where ρ is the mass density, σ the Cauchy stress tensor and **f** the body force per unit mass. The additional body for $\mathbf{f}^{\mathrm{m}}$ and the body couple $\mathbf{L}^{\mathrm{m}}$ are due to the magnetization of the body and with the assumption of static fields acting on electrically nonpolarized stationary magnetic materials they are given by [23]

$$\rho \mathbf{f}^{m} = \mu_o (\nabla \mathbf{H}) \mathbf{M} \text{ , and } \rho \mathbf{L}^{m} = \operatorname{skw} \left(\mu_o \mathbf{M} \otimes \mathbf{H} \right). \tag{7}$$

By defining the Maxwell stress tensor as [15,23]

$$\sigma^{\mathbf{M}} = \mu_o \mathbf{H} \otimes \mathbf{H} + \mu_o \mathbf{H} \otimes \mathbf{M} - \frac{1}{2} \mu_o \left(\mathbf{H} \cdot \mathbf{H} \right) \mathbf{I}, \tag{8}$$

the equilibrium equations (6) can be rewritten as

$$\nabla \cdot \left(\sigma + \sigma^{\mathbf{M}} \right) + \rho \mathbf{f} = 0 \quad \text{in } \Omega, \tag{9a}$$

$$\operatorname{skw} \left(\sigma + \sigma^{\mathrm{M}} \right) = 0 \text{ in } \Omega, \tag{9b}$$

The following jump conditions apply at all interfaces

$$[[\sigma + \sigma^{\mathbf{M}}]] \cdot \mathbf{n} \quad \text{on } \partial\Omega. \tag{10}$$

The remaining equations to complete the formulation of the magnetomechanical boundary value problem for MSMAs are the constitutive relations, which are specified in a following section.

The coupling between the mechanical and the magnetostatic problem has several contributions to the magnetostatic boundary value problem:

1. Constitutive relations: The magnetization in Eqn. (3), for example, is not only a function of the magnetic field, but also the applied stress and the loading history through a set of internal state variables ζ. The relation **M** = **M**(σ, **H**, ζ) is provided by the constitutive model to be introduced shortly.
2. Body force and body couple (7), captured through Maxwell's stress tensor (8), introduce magnetic field dependence into the equilibrium equations (9).
3. Coupled boundary conditions (10).
4. Deformations of the body, resulting in configurational changes, affect the solution of the magnetostatic problem (3).

3. THE COUPLING BETWEEN THE MECHANICAL AND THE MAGNETOSTATIC PROBLEM

In order to determine the effect of the magnetic body force on the equilibrium equations, the finite element software package COMSOL Multiphsysics was used to calculate the magnetic body force. The COMSOL model used represented a typical experiment which consists of subjecting a martensitic MSMA parallelepiped sample to a constant mechanical load (traction) on two opposing faces of the boundary and subsequently to a perpendicular magnetic field. The geometry of the boundary value problem to be solved is determined by considering typical sample dimensions of 8 mm x 4 mm x 4 mm, or aspect ratios of 2:1:1, with respect to the axial load direction x, the applied field direction y and the remaining transverse direction z, as shown in Fig. 1. Due to the numerical complexity of the problem and for illustration purposes, however, the analysis is performed in two-dimensions, which, with an in-plane aspect ratio of 2:1, essentially assumes that the specimen extends to infinity in the z-direction. All of the conclusions that will be drawn from this analysis, however, are generalizable to three dimensions. According to the electromagnet specification, a uniform magnetic field can be assumed in a gap of the dimensions 26 mm x 26 mm x 26 mm. For the numerical analysis of the magnetostatic problem (3), subject to the jump conditions (2), the finite element mesh depicted in Fig. 1 is used. This figure also indicates the location of the specimen and the nonmagnetic grips (dashed lines). A constant magnetic flux of $B_y^{\text{applied}} = \mu_o H_y^{\text{applied}}$ is applied on the boundary.

In order to find the body force due to magnetization, the internal magnetic field and magnetization of the specimen are needed. These quantities are output data from the COMSOL model, which has also as input the constitutive material response for the MSMA presented in the next section,

in addition to geometry and boundary conditions. The gradient of the magnetic field operating on the magnetization vector is averaged over the specimen to result in the magnetic body force according to Eqn (7).

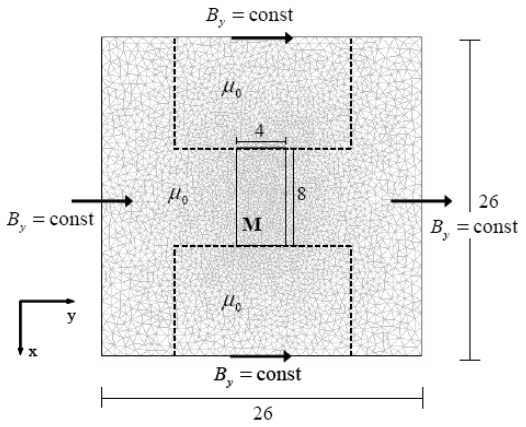

Figure 1: Domain geometry, mesh and boundary conditions for the magnetostatic problem. Dashed lines indicate the location of the nonmagnetic grips of the load frame.

The maximum average body force due to magnetization found for different applied magnetic fields was 0.22 N/m^3, as shown in Fig. 2. Relatively, the magnetic body force is negligible in the way it influences the equilibrium equations and gives rise to stresses, compared to the applied mechanical tractions.

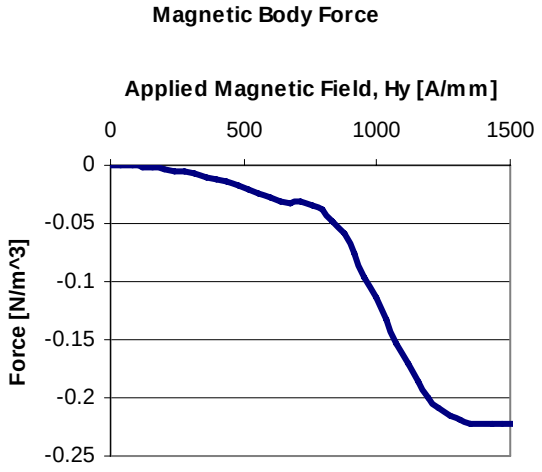

Figure 2. Maximum average magnetic body force magnitude as a function of the applied magnetic field.

The magnetic shape memory effect occurs for applied tractions resulting in stress ranges for the MSMA specimen between 1 and 10 MPa, while the average stress due to the magnetic body force (Maxwell stress) is approximately 0.05 MPa, which is comparatively very small. It is worth noting that a very small Maxwell's stress will also have an insignificant impact on the conservation of angular momentum equations (Eqns 9b).

4. THE MSMA CONSTITUTIVE MODEL

A phenomenological model has been proposed by the authors to describe the stress- and magnetic field-induced reorientation of martensitic variants in MSMAs. Since the focus of this paper is on the magnetostatic boundary value problems, only a brief summary shall be given here and the reader is referred to previous publication for more detail [9,10,23]. The model is based on the Gibbs free energy function G, in which the Cauchy stress tensor σ and the magnetic field strength **H** are the independent state variables. The loading history dependence of the constitutive behavior caused by dissipative effects is introduced through the evolution of internal state variables. The chosen internal state variables are the variant volume fraction ξ, the magnetic domain volume fraction α and the magnetization rotation angles θ_i. These variables are motivated by experimentally observed changes in the crystallographic and magnetic microstructure [25].

The specific form of the Gibbs free energy for the Kiefer and Lagoudas model [9] is given by

$$\begin{aligned} G &= \hat{G}\left(\sigma, \mathbf{H}, \xi, \alpha, \theta_i\right) \\ &= -\frac{1}{2\rho}\sigma : S\left(\xi\right)\sigma - \frac{\mu_o}{\rho}\mathbf{M}\left(\xi,\alpha,\theta_i\right)\cdot\mathbf{H} \\ &+ \mathrm{G}^{an}\left(\xi,\alpha,\theta_i\right) + E^{mix}\left(\xi\right) + \mathrm{G}_o \end{aligned} \qquad (11)$$

where S, $\mathbf{M}^{\mathrm{eff}}$ and G^{an} are the effective compliance tensor and magnetocrystalline anisotropy, respectively. The free energy function (11) is comprised of the elastic strain energy, the Zeeman energy, the magnetocrystalline anisotropy energy, a mixing term and a reference state value. The Zeeman or external field energy aims to align the internal magnetization with the eternally applied magnetic field. The magnetocrystalline anisotropy energy can be viewed as the energy stored in the material due to the work done by rotating the magnetization away from the magnetic easy axes. The mixing term accounts for the deviation of the total free energy from the assumed weighted average of the individual variants and magnetic domains due to interactions.

Different combinations of these energy terms have also been included in other constitutive models [3,26,27]. Unlike most of these formulations,

however, this work is concerned with the influence of dissipative effects on the evolution of thermodynamic states, rater than the minimization of the free energy. This approach has successfully been used in the modeling of conventional shape memory alloys [28,29].

From the free energy expression (11) the constitutive equations are derived in a thermodynamically-consistent manner [9], such that

$$\varepsilon^e = \varepsilon - \varepsilon^r = -\rho \frac{\partial \hat{G}}{\partial \sigma}, \quad \text{and} \quad \mathbf{M} = -\frac{\rho}{\mu_o}\frac{\partial \hat{G}}{\partial \mathbf{H}} \qquad (12)$$

where an additive decomposition of the total strain into an elastic strain and a reorientation strain has been assumed, and the total infinitesimal strain is related to

Table 1: Summary of the reduced model equations for the special case of uniaxial stress and perpendicular magnetic field.

Magnetic Field-Induced Strain and Magnetization:

$$\varepsilon^r_{xx} = \varepsilon^{r,\max}\xi\,; \quad \varepsilon^r_{yy} = -\varepsilon^r_{xx}.$$

$$M_x = (1-\xi)M^{sat}\sqrt{1-\left(\frac{\mu_0 M^{sat}}{4\rho K_1}\right)^2 H_y^2}\,;$$

$$M_y = \xi M^{sat} + (1-\xi)M^{sat}\frac{\mu_0 (M^{sat})^2}{2\rho K_1}H_y\,.$$

Driving Force for Variant Reorientation:

$$\pi^\xi = \sigma\Lambda^r_{xx} - \rho\frac{\partial \hat{G}}{\partial \xi} = \sigma\varepsilon^{r,\max} + \mu_0 M^{sat}H_y - \frac{(\mu_0 M^{sat})^2}{4\rho K_1}H_y^2 - \frac{\partial f^\xi}{\partial \xi}.$$

2.5ex] **Reorientation Function:**

$$\Phi^\xi(\sigma,\mathbf{H},\xi) = \begin{cases} \pi^\xi - Y^{\xi,c}, & \dot{\xi} > 0 \\ -\pi^\xi - Y^{\xi,c}, & \dot{\xi} < 0 \end{cases}.$$

Kuhn-Tucker Loading Conditions:

$$\Phi^\xi(\sigma,\mathbf{H},\xi) \le 0, \quad \Phi^\xi\dot{\xi} = 0\,.$$

Hardening Function (Derivative):

$$\frac{\partial f^{\xi,c}}{\partial \xi} = \begin{cases} -A^c\left[\pi - \cos^{-1}(2\xi-1)\right] + (B_1^c + B_2^c), & \dot{\xi} > 0 \\ -C^c\left[\pi - \cos^{-1}(2\xi-1)\right] + (B_1^c - B_2^c), & \dot{\xi} < 0 \end{cases}.$$

the displacement field by $\varepsilon = \frac{1}{2}\left(\nabla\mathbf{u} - (\nabla\mathbf{u})^T\right)$. A reduced form of the remaining constitutive equations is present in Tab 1. This simplified set of equations holds for a typical loading case in which only the components σ_{xx} and H_y are non-zero. An example of relations between the model parameters and material constants are specified in [9].

Based on these constitutive equations exemplary model predictions of the magnetic field-induced strain and the magnetization response for different constant stress levels are depicted in Fig. 3 and 4, respectively. This particular prediction is based on model parameters calibrated from data published by Heczko et al. 2003 [2]. For more details on these predictions the reader is again referred to [9,10].

Recently the authors have addressed the impact of magnetic domain wall motion at low magnetic fields. As evident from Eqn. (11), the presented MSMA constitutive model already incorporates the magnetic domain volume fraction α as an internal state variable and its relation to the macroscopic magnetization is defined through Eqn. (12). Previously the evolution of magnetic domains had been neglected based on the argument that unfavorable magnetic domains are eliminated as soon as the reorientation process is activated [10,11,30]. This argument can actually only be justified for the forward reorientation process, because it usually occurs at relatively high magnetic fields. The reverse reorientation process, however, occurs at low magnetic fields. In various experiments it has been observed that MSMA typically do not produce remnant magnetization [2,31], although they do exhibit residual strains. If domain wall motion is neglected at moderate to high stresses, with respect to a scale between zero and the blocking stress, the model predicts that the mechanism of reverse variant reorientation returns the magnetization to low values of remnant magnetization, but not zero, as can be seen in Fig. 4.

At very low stress levels this problem becomes much more apparent since the recovery of the stress-favored variant is usually not induced. In this case the model predicts a remnant magnetization of M^{sat}. If one is interested in an accurate prediction of the magnetization behavior of MSMAs at low magnetic field and low stresses and not just accurate predictions of the strain response this is unacceptable. By deriving evolution equations from thermodynamic constraints, similar to those derived for the magnetization rotation angles [10,11], the model was successfully modified to account for the motion of magnetic domain walls in this load regime. An example of reorientation strain and magnetization predictions with magnetic domain wall motion are shown in Figs. 4 and 5.

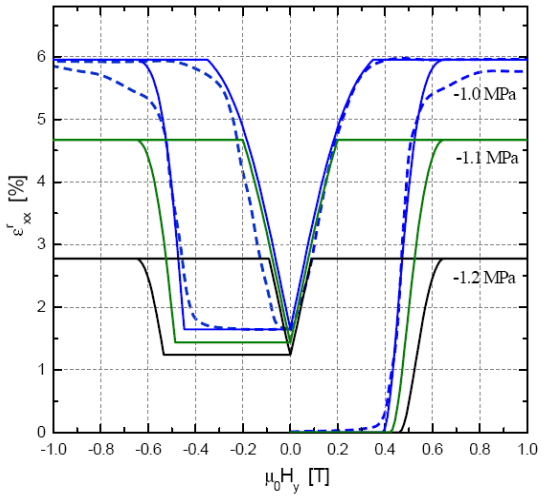

Figure 3: Predicted MFIS hysteresis curves at different stress levels. Solid lines: Model. Dashed lines: Experimental data [2].

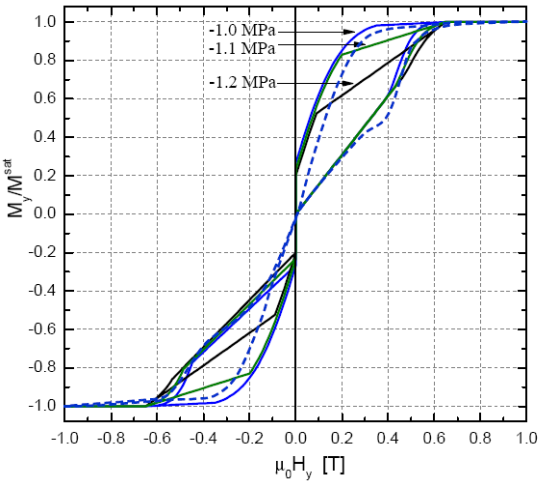

Figure 4: Predicted magnetization curves at different stress levels. Solid lines: model. Dashed line: experimental data [2].

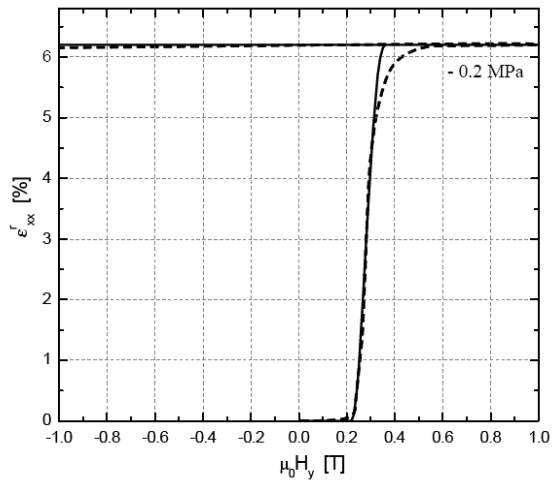

Figure 5: Predicted MFIS hysteresis curve. Solid Lines: Model. Dashed line: Experimental Data [2].

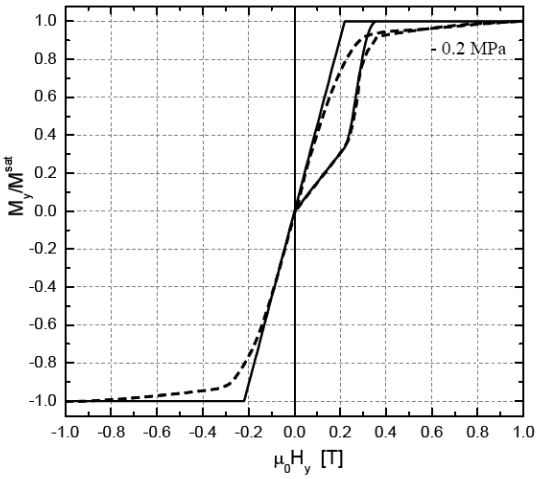

Figure 6: Predicted magnetization curve when accounting for magnetic domain wall motion at low magnetic field and stress levels. Solid lines: Model. Dashed line: Experimental dea [2].

5. DISCUSSION

The main results of the work presented in this paper can be summarized as follows:

1. The body force due to a non-uniform magnetic field in a MSMA specimen was calculated using a multiphysics finite element analysis.
2. The average stress due to the magnetic body force was calculated.
3. The magnetic body force does not have a significant impact on the equilibrium equations compared to the applied mechanical tractions.
4. The stress due to the magnetic body force does not influence the magnetic shape memory effect since its effect is very small compared to the influence of the applied mechanical load on the reorientation of martensitic variants.

ACKNOWLEDGMENTS

This work was supported by the Army Research Office, contract no's. DAAD 19-02-1-0261 and W911NF-06-1-0319, P00002, and the National Science Foundation, grant no's DMR-0244126 and EEC-0453578.

REFERENCES

1. Yamamoto, T., Taya, M., Sutou, Y., Liang, Y., Wada, T., and Sorensen, L., 2004, "Magnetic field-induced reversible variant rearrangement in Fe-Pd single crystals". *Acta Materialia*, **52**(17), pp. 5083-5091.
2. Heczko, O., Straka, L., and Ullakko, K., 2003. "Relation between structure, magnetization process and magnetic shape memory effect of various martensites occurring in Ni-Mn-Ga alloys". *Journal de Physique IV France,* **112**, pp. 959-962.
3. O'Handley, R.C., 1998. "Model for strain and magnetization in magnetic shape-memory alloys'. *Journal of Applied Physics*, **83**(6), pp. 3263-3270.
4. Murray, S. J., Marioni, M., Tello, P. G., Allen, S. M., and O'Handley, R. C., 2001. "Giant magnetic-field-induced strain in Ni-Mn-Ga crystals: Experimental results and modeling". *Journal of Magnetism and Magnetic Materials*, **226-230**(1), pp. 945-947.
5. Müllner, P., Chernenko, V. A., and Kostorz, G., 2003. "A microscopic approach to the magnetic-field-induced deformation of martensite (magnetoplasticity)". *Journal of Magnetism and Magnetic Materials*, **267**, pp. 325–334.
6. Shield, T. W., 2003. "Magnetomechanical testing machine for ferromagnetic shape-memory alloys". *Review of Scientific Instruments*, **74**(9), pp. 4077-4088.
7. Likhachev, A. A., Sozinov, A., and Ullakko, K., 2004. "Different modeling concepts of magnetic shape memory and their comparison with some experimental results obtained in Ni-Mn-Ga". *Material Science &Engineering A*, **378**, pp. 513-518.
8. Kiefer, B., and Lagoudas, D. C., 2004. "Phenomenological modeling of ferromagnetic shape memory alloys". *Proceedings of SPIE, Smart Structure and Materials: Active Materials: Behavior and Mechanics, San Diego, CA, 14-18 March 2004*, **5387**, pp. 164-176.
9. Kiefer, B. and Lagoudas, D. C., 2005. "Magnetic field-induced martensitic variant reorientation in magnetic shape memory alloys". *Philosophical Magazine Special Issue: Recent Advances in Theoretical Mechanics, in Honor of SES 2003 A.C. Eringen Medalist G.A. Maugin*, **85**(33-35), pp. 4289-4329.
10. Kiefer B., and Lagoudas D. C., 2005. "Modeling of the magnetic field-induced martensitic variant reorientation and the associated magnetic shape memory effect in MSMAs". *Proceedings of SPIE, Smart Structures and Materials: Active Materials: Behavior and Mechanics, San Diego, CA, 6-10 March 2005*, **5761**, pp454-465.
11. Kiefer, B., and Lagoudas, D. C., 2006. "Modeling of the hysteretic strain and magnetization response in magnetic shape memory alloys". *Proceedings of AIAA 2006*, **paper 1766**, pp. 1-15.
12. Kiefer, B., and Lagoudas, D. C., 2006. "Application of a magnetic sma constitutive model in the analysis of magnetomechanical boundary value problems". *Proceedings of SPIE, smart Structures and Materials: Active Materials: Behavior and Mechanics, San Diego, CA, 26 February – 2 March, 2006*, **6170**, pp. 330-341.
13. Lagoudas, D. C., Kiefer, B., and Broederdorf, A. J., 2006. "Accurate interpretation of magnetic shape memory alloy experiments utilizing coupled magnetostatic analysis". *Proceedings of ASME, International Mechanical Engineering Congress and Exposition, Chicago, IL, 5-10 November, 2006.*
14. Jackson, J. D., 1975. *Classical Electrodynamics*, 2nd ed. John Wiley & Sons.
15. Woodson, H. H., and Melcher, J. R., 1990. *Electromechanical Dynamics, Part I: Discrete Systems*, Reprint of 1968 ed. Krieger Publishing Company.
16. Bertram, H. N., 1994. *Theory of Magnetic Recording*. Cambridge University Press.
17. O'Handley, R.C., 2000. *Modern Magnetic Materials*. John Wiley & Sons.
18. Cullity, B. D., 1972. *Introduction to Magnetic Materials*. Addison-Wesley.
19. Bozorth, R. M., 1993. *Ferrormagnetism*, reissue of 1951 ed. IEEE Press.
20. Schlömann, E., 1962. "A sum rule concerning the inhomogeneous demagnetizing field in nonellipsoidal samples". *Journal of Applied Physics*, **33**(9), pp. 2825-2826.
21. Moskowitz, R., and Della Torre, E., 1966. "Theoretical aspects of demagnetization tensors". *IEEE Transactions on Magnetics*, **2**(4), pp. 739-744.
22. Eringen, A. C., and Maugin, G. A., 1990. *Electrodynamics of Continua I – Foundations and Solid Media*. Springer-Verlag.
23. Hutter, K., and van de Ven, A. A. F., 1978. *Field Matter Interaction in Terhmoelastic Solids*, Vol. 88 of *Lecture Notes in Physics*. Springer-Verlag.
24. Kiefer, B., Karaca, H. E., Lagoudas, D. C., and Karaman, I., 2006. "Characterization and modeling of the magnetic field-induced strain and work output in Ni_2MnGa shape memory alloys". *Submitted to Journal of Magnetism and Magnetic Materials*.
25. Sullivan, M. R., and Chopra, H. D., 2004. "Temperature- and field-dependent evolution of micromagnetic structure in ferromagnetic shape-memory-alloys". *Physical Review B*, **70**, pp. 094427-(1-8).
26. James, R. D., and Hane, K. F., 2000. "Martensitic transformations and shape-memory materials". *Acta Materialia,* **48**(1) pp. 197-222.
27. Hirsinger, L., and Lexcellent, C., 2003. "Internal variable model for magneto-mechanical behaviour of ferrormagnetic shape memory alloys Ni-Mn-Ga". *Journal de Physique IV France*, **112**, pp. 977-980.
28. Lagoudas, D. C., Bo, Z., and Qidwai, M. A., 1996. "A unified thermodynamics constitutive model for SMA and finite element analysis of active metal matrix composites". *Mechanics of Composite Materials and Structures*, **3**, pp. 153-179.

29. Boyd, J. G., and Lagoudas, D. C., 1996. "A thermodynamical constitutive model for shape memory materials. Part I. The monolithic shape memory alloy". *International Journal of Plasticity,* **12**(6), pp. 805-842.
30. O'Handley, R. C., Allen, S. M., Paul, D. I., Henry, C. P., Marioni, M., Bono, D., Jemkins, C., Banful, A., and Wager, R., 2003. "Keynote address: Magnetic field-induced strain in single crystal Ni-Mn-Ga". *Proceedings of SPIE, Symposium on Smart Structures and Materials,* **5053**, pp. 200-206.
31. Tickle, R., 2000. "Ferromagnetic shape memory materials". PhD thesis, university of Minnesota, May.